



Cite this: *Phys. Chem. Chem. Phys.*,
2015, 17, 4730

Control of selectivity in allylic alcohol oxidation on gold surfaces: the role of oxygen adatoms and hydroxyl species†

Gregory M. Mullen,^a Liang Zhang,^b Edward J. Evans Jr.,^b Ting Yan,^b
Graeme Henkelman^b and C. Buddie Mullins^{*abc}

Gold catalysts display high activity and good selectivity for partial oxidation of a number of alcohol species. In this work, we discuss the effects of oxygen adatoms and surface hydroxyls on the selectivity for oxidation of allylic alcohols (allyl alcohol and crotyl alcohol) on gold surfaces. Utilizing temperature programmed desorption (TPD), reactive molecular beam scattering (RMBS), and density functional theory (DFT) techniques, we provide evidence to suggest that the selectivity displayed towards partial oxidation *versus* combustion pathways is dependent on the type of oxidant species present on the gold surface. TPD and RMBS results suggest that surface hydroxyls promote partial oxidation of allylic alcohols to their corresponding aldehydes with very high selectivity, while oxygen adatoms promote both partial oxidation and combustion pathways. DFT calculations indicate that oxygen adatoms can react with acrolein to promote the formation of a bidentate surface intermediate, similar to structures that have been shown to decompose to generate combustion products over other transition metal surfaces. Surface hydroxyls do not readily promote such a process. Our results help explain phenomena observed in previous studies and may prove useful in the design of future catalysts for partial oxidation of alcohols.

Received 17th October 2014,
Accepted 7th January 2015

DOI: 10.1039/c4cp04739g

www.rsc.org/pccp

Introduction

Selective partial oxidation reactions involving conversion of alcohols to corresponding ketones, aldehydes, or carboxylic acids are challenging chemical processes. Current industrial techniques utilize hazardous transition metal oxides as stoichiometric reactants. Handling and disposal of these materials creates a number of environmental issues. The development of a catalytic alternative for partial oxidation of alcohols could help alleviate these concerns. Gold catalysts display high activity for a number of reactions,^{1–3} including partial oxidation of alcohols,^{4–7} offering a promising alternative to current industrial methods.

Generally, gold catalysts display high activity for partial oxidation reactions in basic aqueous media.^{6,8} The reaction mechanism for such processes has been suggested to involve

the production of an aldehyde intermediate species with subsequent oxidation of the aldehyde yielding a carboxylic acid.⁵ The initial oxidation reaction associated with transformation of the alcohol species to the aldehyde has been proposed to be the rate-determining step for this process.⁹

Most gold catalysts only display high activity for partial oxidation of alcohols under basic aqueous conditions.^{6,8} However, some catalysts consisting of gold nanoparticles supported on ceria (Au/CeO₂)¹⁰ can effectively promote partial oxidation in the pure alcohol phase. Cationic sites (Ce³⁺ and Au⁺) at the interface between the gold particles and the ceria support have been suggested to promote activity on this catalyst by facilitating hydride removal from the reactive intermediate.¹⁰ However, this mechanism has yet to be confirmed, and the reasons for the high activity displayed by Au/CeO₂ remain under debate.

Allylic alcohols contain C=C bonds, which can influence their reactivity and selectivity towards catalytic processes. While simple alcohols can be oxidized to their corresponding aldehydes with high selectivity over Au–Pd/TiO₂ catalysts,^{11,12} the selectivity towards partial oxidation of allylic alcohols displayed on these catalysts is limited by a number of parallel reactions, including isomerization, hydrogenation, and polymerization.¹² In contrast, Au/CeO₂ catalysts have demonstrated high activity and high selectivity for the partial oxidation of allylic alcohols to aldehydes.^{12,13} A fundamental mechanistic understanding of

^a McKetta Department of Chemical Engineering, University of Texas at Austin, Austin, Texas 78712-0231, USA. E-mail: mullins@che.utexas.edu

^b Department of Chemistry, University of Texas at Austin, Austin, Texas 78712-0231, USA

^c Center for Nano and Molecular Science and Technology, Texas Materials Institute, and Center for Electrochemistry, University of Texas at Austin, Austin, Texas 78712-0231, USA

† Electronic supplementary information (ESI) available. See DOI: 10.1039/c4cp04739g

the interactions between allylic alcohols and oxidant species on the gold surface may help explain this behavior and guide future catalyst development.

Surface science studies carried out on model gold catalysts under ultrahigh vacuum (UHV) conditions have advanced fundamental understandings of gold-adsorbate interactions.^{14–22} Previous studies have investigated oxidation of allylic alcohols on O/Au(111)^{23–25} and Au/Pd(111) surfaces.²⁶ Lee *et al.* found that incorporating small amounts of gold into the Pd(111) surface improved selectivity for the partial oxidation of crotyl alcohol to crotonaldehyde by suppressing side reaction pathways.²⁶ In a series of studies, Friend and coworkers investigated the interactions of allylic alcohols with oxygen adatoms on the Au(111) surface.^{23,24} Various oxidation reactions were promoted on the gold surface, resulting in the generation of several products.^{23,24}

We previously investigated the partial oxidation of allyl alcohol to acrolein on the O/Au(111) surface ($\text{CH}_2=\text{CHCH}_2\text{OH} + \text{O} \rightarrow \text{CH}_2=\text{CHCHO} + \text{H}_2\text{O}$).²⁵ This process can occur *via* multiple reaction mechanisms (depicted in Scheme 1), which are dictated by the relative coverage of oxygen adatoms and hydroxyls on the gold surface. The reaction is initiated by removal of the hydroxyl hydrogen from allyl alcohol *via* an oxygen adatom (Scheme 1a), resulting in the generation of an alkoxide intermediate and a surface hydroxyl. Hydroxyls on the gold surface can also facilitate this process, producing the alkoxide and water (Scheme 1b). Both of these processes are facile, occurring with very low activation barriers (E_a), which are shown in Scheme 1, as determined *via* density functional theory (DFT) calculations.²⁵ Acrolein is

generated by α -dehydrogenation of the alkoxide intermediate, which can also be promoted by either an oxygen adatom (Scheme 1c) or a hydroxyl species with a second alkoxide mediating the process (Scheme 1d). The oxygen-promoted α -dehydrogenation process is facile, occurring with a very low E_a . α -Dehydrogenation *via* a surface hydroxyl occurs *via* a more energetic process which is lowered by the participation of a second alkoxide species. This work²⁵ elucidated the mechanism for partial oxidation of allyl alcohol to acrolein on the gold surface. However, the factors governing the selectivity towards the various oxidation pathways that can be facilitated on the gold surface remain unknown. Understanding these factors could prove useful in tailoring catalyst design. The current work builds upon this previous study²⁵ by exploring other oxidative pathways promoted on O/Au(111) surfaces and the mechanistic factors that dictate selectivity towards each pathway.

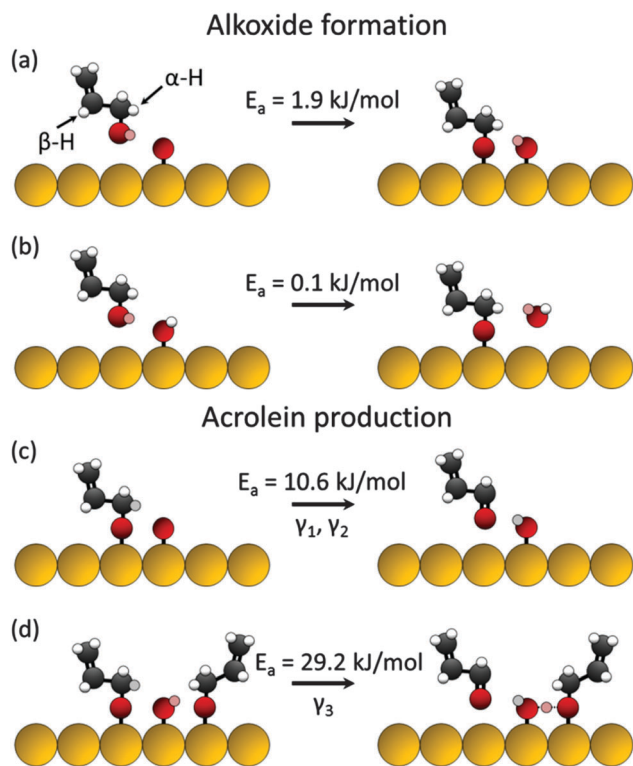
The presence of water and/or hydroxyls may influence the selectivity displayed by gold surfaces for alcohol oxidation reactions. Incorporation of water into the reactant feed stream has been shown to improve the activity of gold catalysts for a number of reactions,^{8,27} including CO oxidation,^{28–31} propene epoxidation,^{32–34} and reduction of nitric oxide with propene.³⁵ Furthermore, Zope *et al.* suggested that hydroxyls are responsible for facilitating partial oxidation of ethanol and glycerol on the gold surface after observing incorporation of isotopically labeled oxygen into product species. This reaction required the presence of O_2 as well, but O_2 was suggested to be responsible for scavenging electrons from the catalyst surface to regenerate hydroxyls and close the catalytic cycle.³⁶ These studies^{8,36} suggest that hydroxyls present in the solution phase may play an important role in partial oxidation reactions of alcohols on gold catalysts.

In the current study, we explore the trends in selectivity displayed for oxidation of allylic alcohols (allyl alcohol and crotyl alcohol) to various products on O/Au(111) surfaces. Both alcohols were partially oxidized to their corresponding aldehydes with nearly 100% selectivity on the Au(111) surface at low oxygen coverage. At higher oxygen coverages, combustion was observed in addition to partial oxidation. TPD and reactive molecular beam scattering (RMBS) results suggest that hydroxyl species generated as intermediates during the reaction on the gold surface promote the partial oxidation reaction with high selectivity. The decrease in selectivity observed at higher oxygen coverages can be attributed to reaction pathways facilitated by oxygen adatoms, which can promote both partial oxidation and combustion as suggested by DFT calculations.

Experimental and computational methods

UHV experiments

The experiments discussed in this study were carried out in a UHV chamber that has been described in detail previously.^{37,38} A thin Au(111) single crystal sample, cut into a circular disk ~11 mm in diameter and 1.5 mm thick, is mounted to a tantalum plate that can be resistively heated to 900 K with a DC



Scheme 1 Mechanistic pathways for partial oxidation of allyl alcohol to acrolein on O/Au(111) surfaces.²⁵

power supply regulated by a proportional–integral–differential controller. The gold sample is also in thermal contact with a liquid nitrogen reservoir for cooling to a minimum temperature of 77 K. The sample temperature was monitored with a K-type thermocouple spot welded to the tantalum plate. Prior to each experiment, the gold surface was cleaned by exposure to atomic oxygen at 77 K, followed by annealing to 700 K. Cleanliness was routinely verified by Auger electron spectroscopy (AES). Periodically, the surface was sputtered by Ar⁺ ion bombardment at room temperature to remove impurities followed by annealing to 800 K for 10 minutes to restore the structure of the (111) surface.

Analyses were carried out in a scattering chamber with a base pressure of less than 1×10^{-10} Torr. This chamber is equipped with a quadrupole mass spectrometer (QMS) and AES. Reactants were delivered to the Au(111) sample *via* a supersonic molecular beam dosing apparatus consisting of four differentially pumped subchambers. Oxygen atoms were dosed onto the gold sample *via* a radio frequency powered plasma-jet source using a gas mixture of 8% (v/v) O₂ in argon.^{39,40} Oxygen surface coverages were estimated by AES following a method described in a previous study.⁴¹ All reactant species were dosed onto the sample through the same nozzle and beam apertures to ensure coincident exposure.

Temperature programmed desorption (TPD) spectra were obtained by heating the Au(111) sample at 2 K s^{-1} while monitoring m/z signals corresponding to the desorption of various species *via* QMS. For oxidation experiments, oxygen atoms were dosed onto the gold surface first, followed by the alcohol species. Isotopic oxygen (¹⁸O) was employed in some of these experiments to enhance the sensitivity towards features associated with carbon dioxide generation, as the signal to noise ratios for C¹⁶O¹⁸O ($m/z = 46$) and C¹⁸O₂ ($m/z = 48$) were higher than the ratio for C¹⁶O₂ ($m/z = 44$) due to the presence of C¹⁶O₂ in the background of the UHV system. Additionally, the use of ¹⁸O allowed us to observe water production features ($m/z = 20$) in TPD spectra without interference from water desorbed from the walls of the UHV chamber ($m/z = 18$), as discussed in a previous work.²⁵

RMBS spectra were obtained by monitoring product and reactant species *via* QMS while impinging allyl alcohol onto the O/Au(111) surface held at a constant sample temperature. In each of these experiments, atomic oxygen was dosed onto the Au(111) surface at 77 K. The surface was then heated to the specified temperature prior to impingement of a pure molecular beam of allyl alcohol. Under these conditions we estimate translational energy of allyl alcohol molecules to be approximately 0.1 eV and the trapping probability to be unity.^{38,42–46} At temperatures above $\sim 120 \text{ K}$ there will be a kinetic competition for trapped molecules to either desorb or react with oxygen on the surface.^{45,47–49}

Allyl alcohol (ACROS, 99%), ¹⁶O₂ (Matheson Trigas, 99.99%), ¹⁸O₂ (Isotec, 99%), and Ar (Matheson Trigas, 99.9%) were used as received, without further purification.

DFT calculations

DFT calculations were performed with the Vienna ab initio Simulation Package.^{50–53} The interaction between the ionic core and the valence electrons was described by the projector-augmented wave

method⁵⁴ and the valence electrons with a plane-wave basis up to an energy cutoff of 280 eV. A higher cutoff energy of 400 eV resulted in variations of less than 0.005 eV to calculated energy barriers. The exchange correlation contribution to the total energy functional was determined using the functional optB86b-vdW that includes van der Waals (vdW) interactions directly in its functional form by Klimeš *et al.*⁶⁵ The locations and energies of the transition states were calculated with the climbing-image nudged elastic band method.^{55,56} Spin polarization was tested and applied when necessary. The gold surface was modeled as a (3×3) Au(111) slab with 4 atomic layers and 14 Å of vacuum. The Brillouin zone was sampled using a $4 \times 4 \times 1$ Monkhorst–Pack k -point mesh.⁵⁷ The convergence criteria for the electronic structure and the atomic geometry were 10^{-5} eV and 0.01 eV Å^{-1} , respectively.

Results and discussion

Fig. 1 displays TPD spectra for acrolein and C¹⁶O¹⁸O production, the respective products of partial oxidation and combustion of allyl alcohol, obtained in a set of experiments in which allyl alcohol was oxidized on the Au(111) surface precovered with varying amounts of ¹⁸O. Acrolein production and C¹⁶O¹⁸O production were observed by monitoring $m/z = 56$ and $m/z = 46$, the parent masses of each species, respectively. Acrolein production was observed on the 0.02 ML O/Au(111) surface, as shown in Fig. 1a. This process also resulted in the production of water, shown in Fig. S1 of the ESI.† Production of C¹⁶O¹⁸O was not observed for TPD of allyl alcohol on the 0.02 ML O/Au(111) surface. A number of other possible oxidation, decomposition, coupling, and hydrogenation products were also monitored for the TPD experiment at this oxygen coverage. These additional spectra are included in Fig. S1 and S2 of the ESI.† Production signals were not observed for any species other than acrolein and water on the 0.02 ML O/Au(111) surface. An AES spectrum taken immediately after this TPD experiment was identical to that of the clean Au(111) surface, shown in Fig. S3 of the ESI,† suggesting that neither carbon nor oxygen remained on the surface after TPD. These TPD and AES results suggest that allyl alcohol did not decompose or undergo any reaction apart from partial oxidation on the 0.02 ML O/Au(111) surface. Acrolein was generated with $\sim 100\%$ selectivity. This behavior is consistent with the high selectivity displayed by Au/CeO₂ catalysts for partial oxidation of allylic alcohols.¹²

The features displayed in the TPD spectra for acrolein production shown in Fig. 1a varied with oxygen coverage. The high temperature feature, labeled γ_3 in Fig. 1a, has been previously shown to result from α -dehydrogenation of the surface alkoxide intermediate *via* a hydroxyl species as shown in Scheme 1d.²⁵ Although hydroxyls were not initially present on the O/Au(111) surfaces in these experiments, hydroxyls are generated as intermediate species *via* the interaction of the alcohol species with surface oxygen adatoms. As the γ_3 feature was the only acrolein production feature observed for the TPD experiment on the 0.02 ML O/Au(111) surface, it is likely that all

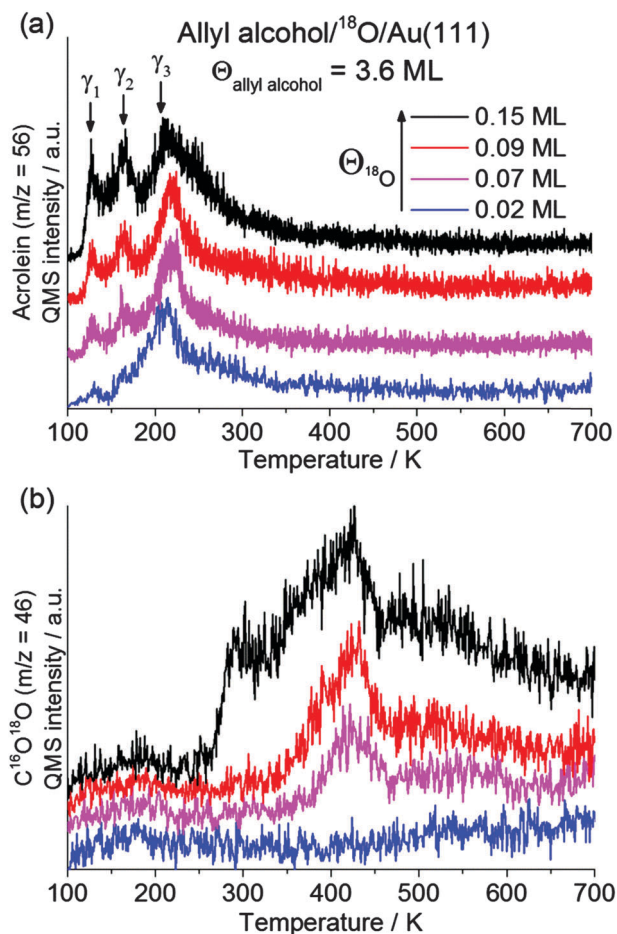


Fig. 1 TPD spectra displaying production of (a) acrolein ($m/z = 56$) and (b) $C^{16}O^{18}O$ ($m/z = 46$) following adsorption of 3.6 ML of allyl alcohol on the Au(111) surface precovered with varying amounts of ^{18}O . Allyl alcohol and ^{18}O were both adsorbed at a sample temperature of 77 K.

of the oxygen adatoms initially present on this surface were converted to hydroxyl species *via* the alkoxide formation process. We would expect that the diffuse coverage of oxygen adatoms relative to allyl alcohol on the surface during this experiment would favor the complete conversion of oxygen adatoms to surface hydroxyl species. After the hydroxyl dehydrogenation step oxygen adatoms would no longer be present on the surface to react with the intermediate species or the acrolein product.

We observed the γ_3 acrolein production feature at every oxygen coverage tested in Fig. 1, and this feature did not change significantly as oxygen coverage was varied. The low and intermediate temperature features, labeled γ_1 and γ_2 in Fig. 1a only appeared on surfaces with oxygen coverages in excess of 0.02 ML. These features are both due to α -dehydrogenation of the alkoxide intermediate *via* oxygen adatoms (Scheme 1c).²⁵ Production of $C^{16}O^{18}O$, indicative of combustion, was also only evident on surfaces with oxygen coverages in excess of 0.02 ML, as shown in Fig. 1b. On these surfaces we would expect oxygen adatoms to encounter and interact with intermediate species on the surface, as γ_1 and γ_2 acrolein production pathways require this interaction. Acrolein produced *via* the partial

oxidation reaction may also interact further with oxygen adatoms on these surfaces. The observation of CO_2 production at the onset of these partial oxidation pathways suggests that oxygen adatoms may be responsible for facilitating combustion in addition to partial oxidation.

In addition to not appearing for TPD of allyl alcohol on the 0.02 ML O/Au(111) surface, the carbon dioxide production features and the γ_1 and γ_2 acrolein production features also propagated in similar monotonic manners as the coverage of oxygen was increased, as shown in Fig. 1. For a more quantitative comparison, we integrated these features and plotted them together in a common graph, shown in Fig. 2. To integrate the γ_1 and γ_2 acrolein production features individually, deconvolution of the spectra in Fig. 1a was necessary. Deconvoluted spectra are shown in Fig. S4 of the ESI.† Fig. 2 plots the sum of the integral areas for the γ_1 and γ_2 features against the integral area for the CO_2 feature at each oxygen coverage. A linear correlation was observed between these integrals, suggesting that a relationship exists between the γ_1 and γ_2 acrolein production pathways and the combustion pathway. Since the γ_1 and γ_2 features for acrolein production have been previously attributed to partial oxidation of the alkoxide intermediate *via* oxygen adatoms,²⁵ the correlation shown in Fig. 2 can be explained by oxygen adatoms promoting both partial oxidation and combustion of the alkoxide intermediate. The γ_3 feature, on the other hand, did not propagate as the oxygen coverage was increased, as shown in Fig. S5 of the ESI.†

To investigate this behavior further, we carried out a set of RMBS experiments on the Au(111) surface at two different oxygen precoverages (Fig. 3). These experiments allow surface dynamics to be probed at a specific temperature. In each experiment atomic oxygen was dosed onto the gold surface at

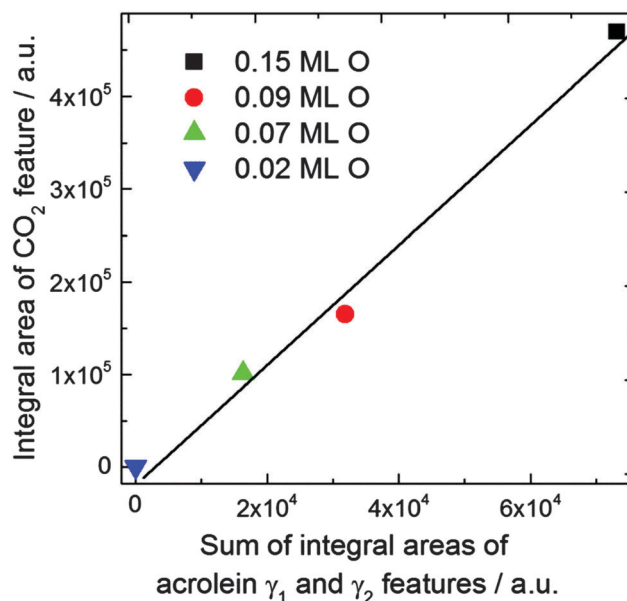


Fig. 2 Integrals for $C^{16}O^{18}O$ features and the sum of acrolein γ_1 and γ_2 features for spectra displayed in Fig. 1. Deconvolution of the features in the acrolein production spectra is shown in Fig. S4 (ESI†).

77 K. The surface was then heated to 350 K prior to impingement of allyl alcohol. At this temperature both partial oxidation and combustion pathways are accessible. Additionally, 350 K is below the temperature at which oxygen adatoms recombine on the Au(111) surface to desorb as O₂.

During impingement of allyl alcohol we monitored production of acrolein and carbon dioxide (C¹⁶O₂) and desorption of allyl alcohol. In these experiments allyl alcohol desorption was observed by monitoring $m/z = 57$, the primary mass fragment of allyl alcohol, and CO₂ production was observed by monitoring $m/z = 44$, the parent mass of CO₂. Fig. 3a displays a RMBS experiment in which allyl alcohol was impinged onto the 0.15 ML O/Au(111) surface. Production signals for both acrolein and CO₂ were detected immediately upon impingement, which began at time = 10 s in Fig. 3a. The peak for CO₂ production was

observed after ~1 second of impingement (time = 10.9 s), while the peak for acrolein production was not observed until ~2 seconds of impingement (time = 11.8 s). In this experiment, the gold surface was initially populated exclusively with oxygen adatoms. Upon impingement of allyl alcohol onto the surface, oxygen was consumed by combustion and *via* the processes depicted in Schemes 1a and c. The decrease in CO₂ production, indicative of combustion, observed after 1 s of allyl alcohol impingement can be attributed to the decrease in surface oxygen adatom coverage brought about by these processes. The time delay between the peaks for CO₂ production and acrolein production can be explained by the participation of the hydroxyl species in the partial oxidation reaction *via* the mechanism shown in Scheme 1d. The increase in hydroxyl coverage brought about by the reaction of oxygen adatoms with allyl alcohol would allow partial oxidation to continue to increase as oxygen was consumed. This behavior is in agreement with the TPD results shown in Fig. 1 and also supports a mechanism whereby oxygen adatoms promote both partial oxidation and combustion of allyl alcohol on the gold surface while hydroxyl species are selective towards partial oxidation.

Fig. 3b displays another RMBS experiment in which allyl alcohol was impinged onto the 0.61 ML O/Au(111) surface. In this experiment, similar behavior was observed with respect to the peaks for CO₂ and acrolein production. Namely, both combustion and partial oxidation began immediately upon impingement of allyl alcohol, and the peak for CO₂ production was observed before the peak for acrolein production. The higher oxygen coverage (0.61 ML) relative to the experiment in Fig. 3a (0.15 ML) allowed CO₂ production to be sustained for a longer period of time, displaying a peak after ~5 s of impingement. The time delay between the CO₂ production peak and the acrolein production peak was also extended from 1 s on the 0.15 ML O/Au(111) surface to ~5 s on this surface.

We performed DFT calculations to investigate a mechanism by which oxygen adatoms on the gold surface can initiate combustion. While determining a complete mechanism for the combustion process would be the ideal case, the number of potential reaction pathways through which the alkoxide intermediate can proceed rendered such an investigation unfeasible in this study. Previous studies^{58,59} have suggested that selective cleavage of an α C-H bond from the process leads to high selectivity for aldehyde formation, whereas nonselective C-H bond cleavage ultimately leads to other oxidative pathways. Therefore, we first investigated the energetics associated with direct β -dehydrogenation of the alkoxide intermediate *via* oxygen atoms on the Au(111) surface, as shown in Fig. 4. However, we found the energy barrier for this process to be 96.0 kJ mol⁻¹, far higher than those associated with partial oxidation of allyl alcohol,²⁵ which are displayed in Scheme 1. We also investigated the energetics associated with β -dehydrogenation from the alkoxide intermediate *via* a hydroxyl species on the Au(111) surface (Fig. 4). This process also has a high activation barrier of 111.9 kJ mol⁻¹. Therefore, we suggest that direct β -dehydrogenation of the alkoxide intermediate is an unlikely initiation step for combustion of allyl alcohol on this surface.

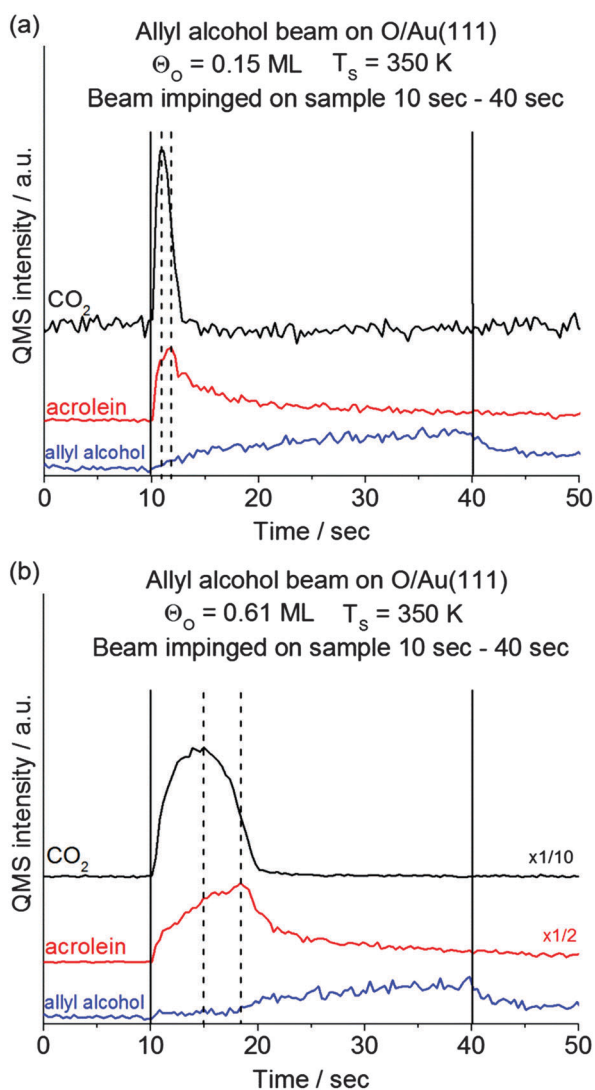


Fig. 3 RMBS of allyl alcohol on the (a) 0.15 ML O/Au(111) surface and (b) 0.61 ML O/Au(111) surface. Allyl alcohol was dosed at a surface temperature of 350 K while monitoring the production of acrolein ($m/z = 56$) and CO₂ ($m/z = 44$) and the desorption of allyl alcohol ($m/z = 57$) *via* QMS. Oxygen adatoms were dosed at a surface temperature of 77 K. The flux of allyl alcohol onto the surface was 0.17 ML s⁻¹.

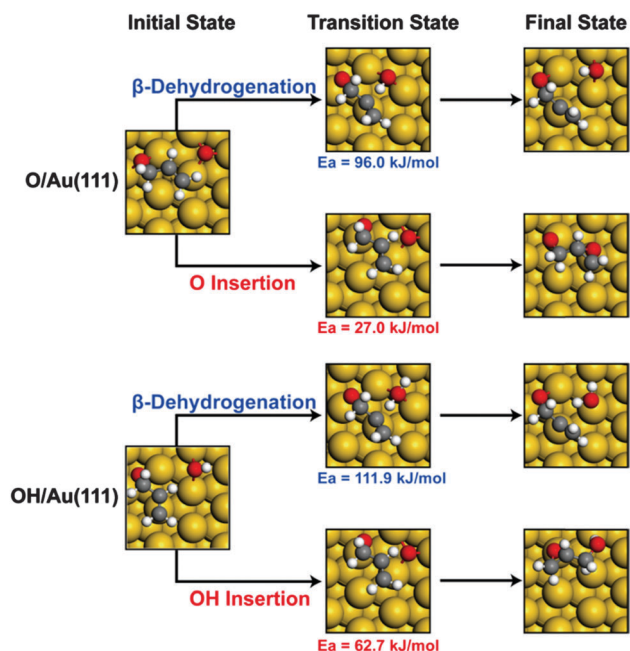


Fig. 4 Reaction pathways associated with potential initiation steps for combustion of the alkoxide intermediate on O/Au(111) and OH/Au(111) surfaces. Activation barriers and atomic structures were determined via DFT calculations.

Another process through which oxygen adatoms may initiate combustion is *via* insertion into the C=C bond of the alkoxide. This process would weaken the C=C bond, which could destabilize the intermediate, facilitating its decomposition into hydrocarbon fragments and/or carbon deposits on the surface which could undergo further oxidation to CO₂. However, the energy barrier for insertion of oxygen from the gold surface into the C=C bond, depicted in Fig. 4, was found to be 27.0 kJ mol⁻¹, which is higher in energy than the oxygen-promoted α -dehydrogenation step. Furthermore, this process would generate a surface bound alkoxy-epoxide intermediate species (additional view shown in Fig. S6 of the ESI[†]), which we expect would result in the formation of glycidol, a C3 epoxy-alcohol, and glycidaldehyde, a C3 epoxy-aldehyde *via* low energy pathways. No features were apparent in the spectrum for $m/z = 43$, a significant mass fragment for glycidol and an expected mass fragment of glycidaldehyde, during the TPD experiment in which allyl alcohol was oxidized on the 0.15 ML O/Au(111) surface, as shown in Fig. S7 of the ESI[†], suggesting that neither species was produced and that the alkoxy-epoxide is an unlikely intermediate for the combustion process.

Yet another potential combustion process involves sequential oxidation of acrolein after its production *via* the partial oxidation reaction. To study this potential combustion pathway, we first calculated the energy barrier for insertion of oxygen into the C=O bond of acrolein, a process that has been suggested to be an initiation step for combustion of acetaldehyde⁶⁰ and acetone⁶¹ on silver surfaces. The energy barrier for this process was found to be quite low on the Au(111) surface (3.9 kJ mol⁻¹), as shown in Fig. 5. Furthermore, this process is exothermic,

with a formation energy of -55.0 kJ mol⁻¹, suggesting that the resulting intermediate species would be stabilized on the gold surface. Once formed, removal of the α -hydrogen from this intermediate occurs with an energy barrier of 26.1 kJ mol⁻¹, resulting in the generation of a bidentate surface species.

The interaction of acetaldehyde with oxygen on silver surfaces has been shown to result in the formation of ethane-1,1-dioxy,^{62,63} a bidentate intermediate that dehydrogenates to generate surface acetate. Surface acetates decompose on the Ag(110) surface in the presence of oxygen at ~400 K to yield combustion products⁶⁴ a temperature very close to what we observed for allyl alcohol combustion on O/Au(111). Therefore, we suggest that a combustion pathway associated with formation of this bidentate intermediate is fitting with the behavior we have observed for allyl alcohol on O/Au(111).

Insertion of a surface hydroxyl species into the C=O bond of acrolein also occurs with a low barrier (5.8 kJ mol⁻¹), as shown in Fig. 5. However, α -dehydrogenation of the resulting species has a far higher activation barrier of 63.7 kJ mol⁻¹, which exceeds that of the reverse barrier for the hydroxyl insertion step (51.1 kJ mol⁻¹), a process that would regenerate acrolein and the surface hydroxyl species. Further oxidation of the intermediate species generated upon insertion of a hydroxyl into the C=O bond of acrolein would therefore be unfavorable if oxygen adatoms are not present on the surface, hindering the combustion process.

Barteau *et al.* showed that a surface acetate intermediate was formed after dosing acetaldehyde onto O/Ag(110) and that some carbon remained on the silver surface after decomposition of this species.⁶⁰ To probe our combustion mechanism further, we carried out AES after the TPD experiment in which 3.6 ML of allyl alcohol was oxidized on the 0.15 ML O/Au(111) surface (Fig. 1). This AES spectrum and a spectrum taken on the clean gold surface are displayed in Fig. 6. A small feature is evident at ~274 eV in the AES spectrum taken after the TPD experiment, marked with a dashed line. This feature corresponds to carbon remaining on the gold surface after the experiment. It is the only apparent difference between the AES spectrum taken post-TPD and that of the clean Au(111) surface. The observation of carbon on this gold surface provides further evidence for our proposed combustion mechanism by analogy to the results of Barteau *et al.* for acetaldehyde oxidation on the O/Ag(110).⁶⁰

We performed a number of TPD experiments in which crotyl alcohol was oxidized on O/Au(111) surfaces, as well. The spectra for these experiments, which are included in the ESI[†], displayed trends in selectivity that are similar to those displayed for allyl alcohol oxidation on O/Au(111) surfaces. The similarities in oxidation behavior between these two allylic alcohols suggests that the selectivity trends observed in this study may extend broadly amongst allylic alcohol species.

Ethanol,⁶⁵ 1-propanol,⁶⁶ 2-propanol,⁶⁶ and 2-butanol⁶⁷ have all been shown to display high selectivity towards production of their corresponding aldehydes in TPD experiments on O/Au(111) surfaces at low oxygen coverages, while both partial oxidation and combustion are observed at higher oxygen coverages.

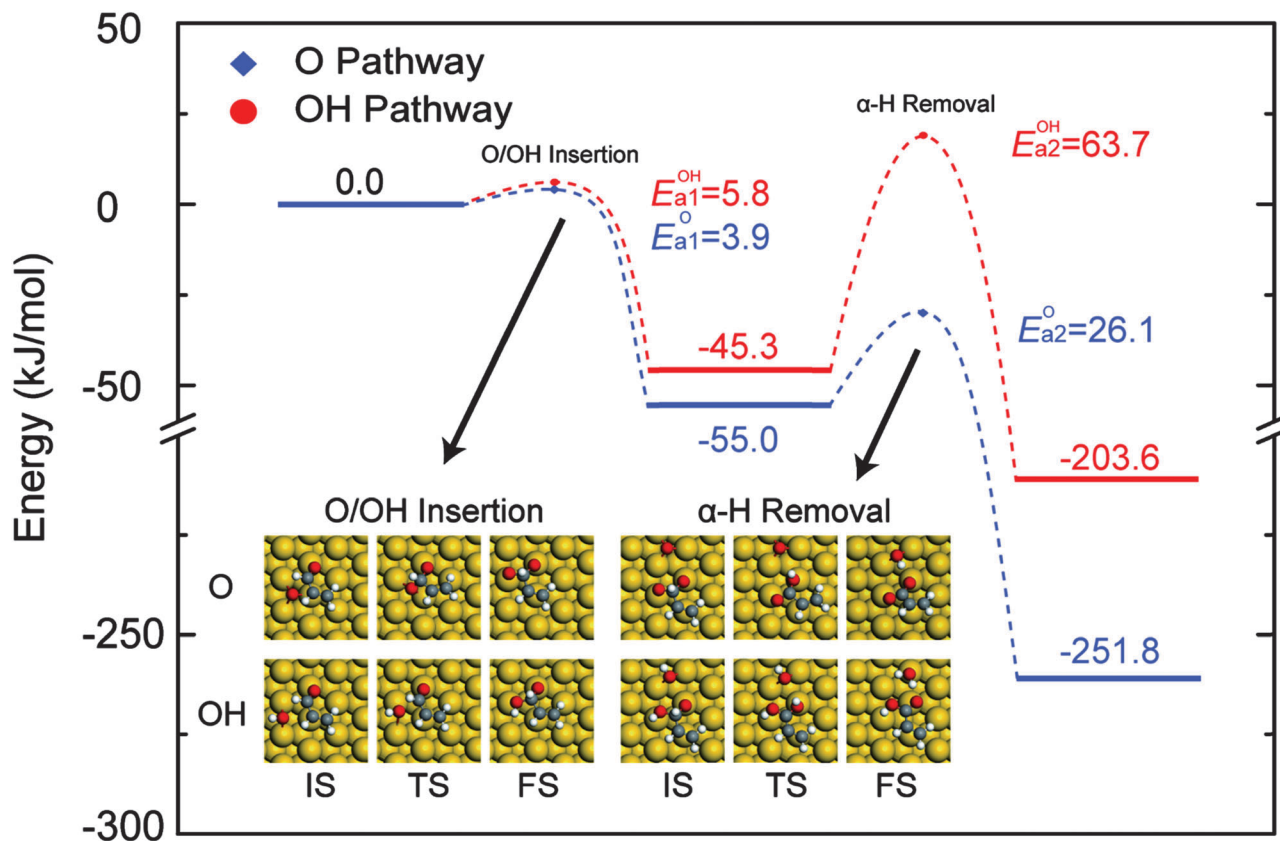


Fig. 5 AES spectra obtained for the clean Au(111) surface (black spectrum) and for the Au(111) surface following TPD of 3.6 ML allyl alcohol on the 0.15 ML O/Au(111) surface (red spectrum). The dashed line indicates an electron energy of 274 eV, the location of an AES feature associated with carbon.

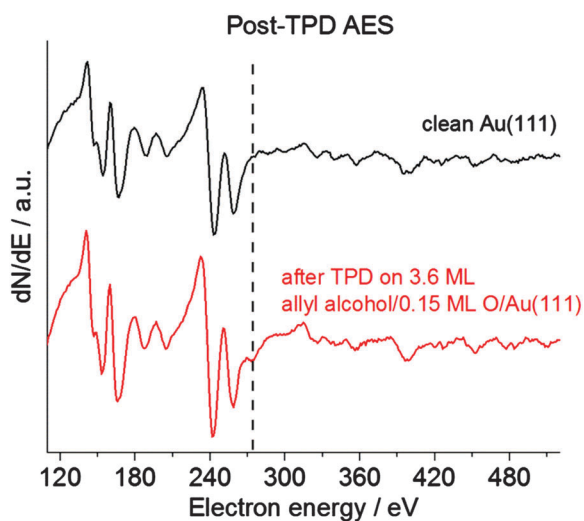


Fig. 6 AES spectra obtained for the clean Au(111) surface (black spectrum) and for the Au(111) surface following TPD of 3.6 ML allyl alcohol on the 0.15 ML O/Au(111) surface (red spectrum). The dashed line indicates an electron energy of 274 eV, the location of an AES feature associated with carbon.

Gong *et al.* suggested that a change in the chemical state of oxygen on the gold surface from chemisorbed oxygen at low coverage to an oxide phase at high coverage might be responsible for the change in product distribution.⁶⁵ The low coverages

and surface temperatures employed during oxygen deposition in our study would not be expected to promote the formation of gold oxide.⁶⁸ The similarities between our results and TPD results for oxidation of other alcohols^{65–67} may suggest that the selectivity effects induced by hydroxyl and oxygen species extend broadly to the oxidation of many alcohol species on gold surfaces.

The participation of hydroxyls in partial oxidation reactions of alcohols on gold surfaces may also help explain observations presented in classical catalysis studies. Abad *et al.* showed that an Au/CeO₂ catalyst could promote the partial oxidation of alcohols to aldehydes in the absence of solvent.¹⁰ In their study, partial oxidation reactions were carried out in neat alcohol and in basic aqueous solutions. Cinnamyl alcohol and 3,4-dimethoxybenzyl alcohol were tested under both sets of conditions, and each species displayed higher conversion and higher selectivity towards partial oxidation products under basic aqueous conditions. A similar conclusion can be drawn from the study by Biella *et al.* in which phenylethane-1,2-diol oxidation was carried out on a gold catalyst.⁶⁹ The authors showed that the selectivity towards the production of mandelic acid, the corresponding carboxylic acid, was enhanced as the pH of the solution was increased. These observations may suggest that hydroxyls play a role in these partial oxidation reactions.

The role of solution phase hydroxyl species in partial oxidation of alcohols was investigated by Zope *et al.*³⁶ The authors of

this study suggested that oxidation of alcohols on the gold surface occurs *via* hydroxyl species. Oxygen (O₂) is required for the reaction to proceed, but the authors suggested that O₂ acts to scavenge free electrons and regenerate the hydroxyl species in solution, closing the catalytic cycle rather than oxidizing the alcohol directly.³⁶ Our results suggest that hydroxyl species on the gold surface can facilitate the partial oxidation of alcohols with high selectivity. Therefore, promotion of the reactions *via* hydroxyl species may account for the high activity and selectivity observed for partial oxidation of alcohols in basic aqueous media.^{6,8}

The promotional effect of water on the partial oxidation of alcohols extends to other transition metals as well. Platinum,^{70,71} palladium,⁷² and ruthenium⁷³ catalysts also demonstrate enhanced activity when in the presence of water. In a DFT study, Chibani *et al.*⁷⁰ showed that hydroxyl groups on the Pt(111) surface, readily generated in the presence of water and oxygen, can promote the partial oxidation of alcohols to their corresponding aldehydes by directly participating in the reaction mechanism. These studies suggest that the influence of water extends beyond catalytic reactions on gold surfaces to other transition metal systems.

Conclusions

We have studied the trends in selectivity displayed on O/Au(111) surfaces towards oxidation reactions involving allylic alcohols. The oxygen precovered gold surface can promote both partial oxidation and combustion pathways. Nearly 100% selectivity towards partial oxidation, resulting in the production of the corresponding aldehydes, was observed when allyl alcohol and crotyl alcohol were oxidized on the gold surface with low oxygen coverage. At higher coverages, combustion was observed in addition to partial oxidation.

TPD and RMBS results suggest that oxygen adatoms are responsible for facilitating both partial oxidation and combustion of allyl alcohol on the gold surface while hydroxyl species, generated as reactive intermediates *via* the interaction of oxygen adatoms with allyl alcohol, are highly selective for the partial oxidation reaction. DFT calculations suggest that a plausible combustion pathway involves the reaction of acrolein with oxygen adatoms on the gold surface to form a bidentate surface intermediate, decomposition of which would be expected to result in combustion products. AES spectra taken immediately after TPD experiments support this conclusion.

Water plays a key role in a number of catalytic reactions. Studies have shown that water can promote catalytic activity for several reactions over various catalysts including partial oxidation of alcohols, and our results suggest that water may also alter reaction pathways, influencing patterns of reactivity displayed by gold catalysts. These observations help explain behavior observed in previous studies and may assist in the design of future catalysts.

Acknowledgements

We are thankful for the generous support of the Department of Energy (DE-FG02-04ER15587 [CBM] and DE-FG02-13ER16428

[GH]) and the Welch Foundation (Grants F-1436 [CBM] and F-1841 [GH]). GMM would like to acknowledge the National Science Foundation for a Graduate Research Fellowship.

Notes and references

- 1 A. S. K. Hashmi and G. J. Hutchings, *Angew. Chem., Int. Ed.*, 2006, **45**, 7896–7936.
- 2 M. Haruta and M. Daté, *Appl. Catal., A*, 2001, **222**, 427–437.
- 3 G. C. Bond and D. T. Thompson, *Catal. Rev.: Sci. Eng.*, 1999, **41**, 319–388.
- 4 L. Prati and M. Rossi, *J. Catal.*, 1998, **176**, 552–560.
- 5 S. E. Davis, M. S. Ide and R. J. Davis, *Green Chem.*, 2013, **15**, 17–45.
- 6 S. Carrettin, P. McMorn, P. Johnston, K. Griffin and G. J. Hutchings, *Chem. Commun.*, 2002, 696–697.
- 7 S. Biella and M. Rossi, *Chem. Commun.*, 2003, 378–379.
- 8 M. S. Ide and R. J. Davis, *Acc. Chem. Res.*, 2013, **47**, 825–833.
- 9 B. Jorgensen, S. E. Christiansen, M. L. D. Thomsen and C. H. Christensen, *J. Catal.*, 2007, **251**, 332–337.
- 10 A. Abad, P. Concepción, A. Corma and H. García, *Angew. Chem., Int. Ed.*, 2005, **44**, 4066–4069.
- 11 D. I. Enache, J. K. Edwards, P. Landon, B. Solsona-Espriu, A. F. Carley, A. A. Herzing, M. Watanabe, C. J. Kiely, D. W. Knight and G. J. Hutchings, *Science*, 2006, **311**, 362–365.
- 12 A. Abad, C. Almela, A. Corma and H. García, *Chem. Commun.*, 2006, 3178–3180.
- 13 A. Abad, A. Corma and H. García, *Pure Appl. Chem.*, 2007, **79**, 1847–1854.
- 14 J. Gong and C. B. Mullins, *Acc. Chem. Res.*, 2009, **42**, 1063–1073.
- 15 J. Gong, *Chem. Rev.*, 2012, **112**, 2987–3054.
- 16 M. Pan, J. Gong, G. Dong and C. B. Mullins, *Acc. Chem. Res.*, 2013, **47**, 750–760.
- 17 M. Pan, A. J. Brush, Z. D. Pozun, H. C. Ham, W.-Y. Yu, G. Henkelman, G. S. Hwang and C. B. Mullins, *Chem. Soc. Rev.*, 2013, **42**, 5002–5013.
- 18 R. J. Madix, C. M. Friend and X. Liu, *J. Catal.*, 2008, **258**, 410–413.
- 19 B. K. Min and C. M. Friend, *Chem. Rev.*, 2007, **107**, 2709–2724.
- 20 J. A. Rodriguez, S. D. Senanayake, D. Stacchiola, P. Liu and J. Hrbek, *Acc. Chem. Res.*, 2013, **47**, 773–782.
- 21 J. A. Rodriguez, *Catal. Today*, 2011, **160**, 3–10.
- 22 J. Gong, D. W. Flaherty, R. A. Ojifinni, J. M. White and C. B. Mullins, *J. Phys. Chem. C*, 2008, **112**, 5501–5509.
- 23 X. Deng, B. K. Min, X. Liu and C. M. Friend, *J. Phys. Chem. B*, 2006, **110**, 15982–15987.
- 24 X. Liu and C. M. Friend, *Langmuir*, 2010, **26**, 16552–16557.
- 25 G. M. Mullen, L. Zhang, E. J. Evans, T. Yan, G. Henkelman and C. B. Mullins, *J. Am. Chem. Soc.*, 2014, **136**, 6489–6498.
- 26 A. F. Lee, S. F. J. Hackett, G. J. Hutchings, S. Lizzit, J. Naughton and K. Wilson, *Catal. Today*, 2009, **145**, 251–257.
- 27 G. M. Mullen, J. Gong, T. Yan, M. Pan and C. B. Mullins, *Top. Catal.*, 2013, **56**, 1499–1511.

- 28 M. Daté, M. Okumura, S. Tsubota and M. Haruta, *Angew. Chem., Int. Ed.*, 2004, **43**, 2129–2132.
- 29 T. Fujitani, I. Nakamura and M. Haruta, *Catal. Lett.*, 2014, **144**, 1475–1486.
- 30 J. Saavedra, H. A. Doan, C. J. Pursell, L. C. Grabow and B. D. Chandler, *Science*, 2014, **345**, 1599–1602.
- 31 G. M. Mullen and C. B. Mullins, *Science*, 2014, **345**, 1564–1565.
- 32 J. Huang, T. Akita, J. Faye, T. Fujitani, T. Takei and M. Haruta, *Angew. Chem., Int. Ed.*, 2009, **48**, 7862–7866.
- 33 S. Lee, L. M. Molina, M. J. López, J. A. Alonso, B. Hammer, B. Lee, S. Seifert, R. E. Winans, J. W. Elam, M. J. Pellin and S. Vajda, *Angew. Chem., Int. Ed.*, 2009, **48**, 1467–1471.
- 34 M. Ojeda and E. Iglesia, *Chem. Commun.*, 2009, 352–354.
- 35 A. Ueda, T. Oshima and M. Haruta, *Appl. Catal., B*, 1997, **12**, 81–93.
- 36 B. N. Zope, D. D. Hibbitts, M. Neurock and R. J. Davis, *Science*, 2010, **330**, 74–78.
- 37 M. C. Wheeler, D. C. Seets and C. B. Mullins, *J. Chem. Phys.*, 1996, **105**, 1572–1583.
- 38 B. A. Ferguson, C. T. Reeves and C. B. Mullins, *J. Chem. Phys.*, 1999, **110**, 11574–11584.
- 39 J. E. Pollard, *Rev. Sci. Instrum.*, 1992, **63**, 1771–1776.
- 40 M. C. Wheeler, D. C. Seets and C. B. Mullins, *J. Chem. Phys.*, 1997, **107**, 1672–1675.
- 41 R. A. Ojifinni, N. S. Froemming, J. Gong, M. Pan, T. S. Kim, J. M. White, G. Henkelman and C. B. Mullins, *J. Am. Chem. Soc.*, 2008, **130**, 6801–6812.
- 42 C. B. Mullins and W. H. Weinberg, *J. Chem. Phys.*, 1990, **92**, 3986–3988.
- 43 C. B. Mullins and W. H. Weinberg, *J. Vac. Sci. Technol., A*, 1990, **8**, 2458–2462.
- 44 C. T. Rettner, C. B. Mullins, D. S. Bethune, D. J. Auerbach, E. K. Schweizer and W. H. Weinberg, *J. Vac. Sci. Technol., A*, 1990, **8**, 2699–2704.
- 45 D. C. Seets, M. C. Wheeler and C. B. Mullins, *Chem. Phys. Lett.*, 1997, **266**, 431–436.
- 46 D. C. Seets, M. C. Wheeler and C. B. Mullins, *J. Chem. Phys.*, 1997, **107**, 3986–3998.
- 47 D. C. Seets, C. T. Reeves, B. A. Ferguson, M. C. Wheeler and C. B. Mullins, *J. Chem. Phys.*, 1997, **107**, 10229–10241.
- 48 C. B. Mullins, C. T. Rettner and D. J. Auerbach, *Chem. Phys. Lett.*, 1989, **163**, 111–115.
- 49 C. B. Mullins and W. H. Weinberg, *J. Chem. Phys.*, 1990, **92**, 4508–4512.
- 50 G. Kresse and J. Hafner, *Phys. Rev. B*, 1993, **47**, 558–561.
- 51 G. Kresse and J. Hafner, *Phys. Rev. B*, 1994, **49**, 14251–14269.
- 52 G. Kresse and J. Furthmüller, *Phys. Rev. B*, 1996, **54**, 11169–11186.
- 53 G. Kresse and J. Furthmüller, *Comput. Mater. Sci.*, 1996, **6**, 15–50.
- 54 P. Blöchl, *Phys. Rev. B*, 1994, **50**, 17953–17979.
- 55 G. Henkelman, B. P. Uberuaga and H. Jónsson, *J. Chem. Phys.*, 2000, **113**, 9901–9904.
- 56 G. Henkelman and H. Jónsson, *J. Chem. Phys.*, 2000, **113**, 9978–9985.
- 57 H. J. Monkhorst and J. D. Pack, *Phys. Rev. B*, 1976, **13**, 5188–5192.
- 58 X. Xu and C. M. Friend, *Surf. Sci.*, 1992, **260**, 14–22.
- 59 J. L. Davis and M. A. Barteau, *Surf. Sci.*, 1988, **197**, 123–152.
- 60 M. A. Barteau, M. Bowker and R. J. Madix, *J. Catal.*, 1981, **67**, 118–128.
- 61 W. S. Sim and D. A. King, *J. Phys. Chem.*, 1996, **100**, 14794–14802.
- 62 W. S. Sim, P. Gardner and D. A. King, *J. Am. Chem. Soc.*, 1996, **118**, 9953–9959.
- 63 M. J. Webb, S. M. Driver and D. A. King, *J. Phys. Chem. B*, 2004, **108**, 1955–1961.
- 64 A. G. Sault and R. J. Madix, *Surf. Sci.*, 1986, **172**, 598–614.
- 65 J. Gong and C. B. Mullins, *J. Am. Chem. Soc.*, 2008, **130**, 16458–16459.
- 66 J. Gong, D. W. Flaherty, T. Yan and C. B. Mullins, *ChemPhysChem*, 2008, **9**, 2461–2466.
- 67 T. Yan, J. Gong and C. B. Mullins, *J. Am. Chem. Soc.*, 2009, **131**, 16189–16194.
- 68 T. A. Baker, X. Liu and C. M. Friend, *Phys. Chem. Chem. Phys.*, 2011, **13**, 34–46.
- 69 S. Biella, L. Prati and M. Rossi, *Inorg. Chim. Acta*, 2003, **349**, 253–257.
- 70 S. Chibani, C. Michel, F. Delbecq, C. Pinel and M. Besson, *Catal. Sci. Technol.*, 2013, **3**, 339–350.
- 71 A. Frassoldati, C. Pinel and M. Besson, *Catal. Today*, 2011, **173**, 81–88.
- 72 Z. Ma, H. Yang, Y. Qin, Y. Hao and G. Li, *J. Mol. Catal. A: Chem.*, 2010, **331**, 78–85.
- 73 X. Yang, X. Wang and J. Qiu, *Appl. Catal., A*, 2010, **382**, 131–137.